

ATP6AP2 functions as a V-ATPase assembly factor in the endoplasmic reticulum

Maria Clara Guida^{a,b,t,‡}, Tobias Hermle^{c,†}, Laurie A. Graham^d, Virginie Hauser^{a,§}, Margret Ryan^d, Tom H. Stevens^d, and Matias Simons^{a,*}

^aImagine Institute, Paris Descartes University–Sorbonne Paris Cité, 75015 Paris, France; ^bGraduate Program GRK1104 and ^cRenal Division, University Medical Center Freiburg, Faculty of Medicine, University of Freiburg, 79106 Freiburg, Germany; ^dDepartment of Chemistry and Biochemistry, Institute of Molecular Biology, University of Oregon, Eugene, OR 97403

ABSTRACT ATP6AP2 (also known as the [pro]renin receptor) is a type I transmembrane protein that can be cleaved into two fragments in the Golgi apparatus. While in *Drosophila* ATP6AP2 functions in the planar cell polarity (PCP) pathway, recent human genetic studies have suggested that ATP6AP2 could participate in the assembly of the V-ATPase in the endoplasmic reticulum (ER). Using a yeast model, we show here that the V-ATPase assembly factor Voa1 can functionally be replaced by *Drosophila* ATP6AP2. This rescue is even more efficient when coexpressing its binding partner ATP6AP1, indicating that these two proteins together fulfill Voa1 functions in higher organisms. Structure–function analyses in both yeast and *Drosophila* show that proteolytic cleavage is dispensable, while C-terminus-dependent ER retrieval is required for ATP6AP2 function. Accordingly, we demonstrate that both overexpression and lack of ATP6AP2 causes ER stress in *Drosophila* wing cells and that the induction of ER stress is sufficient to cause PCP phenotypes. In summary, our results suggest that full-length ATP6AP2 contributes to the assembly of the V-ATPase proton pore and that impairment of this function affects ER homeostasis and PCP signaling.

Monitoring Editor
Howard Riezman
University of Geneva

Received: Apr 23, 2018

Revised: Jun 22, 2018

Accepted: Jul 5, 2018

INTRODUCTION

The vacuolar-type H⁺-ATPase (V-ATPase) consists of a proton pore (V0 sector) and an ATP hydrolysis domain (V1 sector). The biogenesis of the pump begins in the ER with the assembly of the V0 sector under the control of several chaperones (assembly factors). Once assembled, the V0 sector is transported to the Golgi apparatus

where the preassembled V1 sector is added. The fully assembled V-ATPase acidifies the secretory and the endolysosomal pathway thereby providing the adequate pH for proteolytic processing, glycosylation, and protein degradation (Forgac, 2007).

The biochemical purification of the V-ATPase identified ATP6AP1 and ATP6AP2 as accessory subunits (Supek *et al.*, 1994; Ludwig *et al.*, 1998). Yet, more recent findings showed that the transmembrane domain of ATP6AP1 has some sequence homology with the yeast V-ATPase assembly factor Voa1 and that it can partially rescue the growth defect of a yeast strain that is both deficient for Voa1 and harbors mutations in the ER retrieval motif of the assembly factor Vma21 (*voa1::H vma21QQ*) (Jansen *et al.*, 2016a). Interestingly, mutations in both *ATP6AP1* and *ATP6AP2* in humans cause a multisystem disorder with steatohepatitis, immunodeficiency, and psychomotor impairment (Jansen *et al.*, 2016a; Rujano *et al.*, 2017).

Unlike *ATP6AP1*, *ATP6AP2* has been studied in many contexts and species (Peters, 2017). Work in *Drosophila* has suggested that *ATP6AP2* functions as an important factor in the planar cell polarity (PCP) pathway (Buechling *et al.*, 2010; Hermle *et al.*, 2010, 2013), a fundamental morphogenetic program that polarizes cells in the plane of the epithelium. The pathway is best understood in the *Drosophila* pupal wing, where it orchestrates hexagonal cell packing

This article was published online ahead of print in MBoC in Press (<http://www.molbiolcell.org/cgi/doi/10.1091/mbc.E18-04-0234>) on July 11, 2018.

Present addresses: [†]Development, Aging and Regeneration Program, Sanford Burnham Prebys Medical Discovery Institute, La Jolla, CA 92037; [§]Institute for Integrative Biology of the Cell (I2BC), CEA, CNRS, Université Paris Sud, Université, Paris-Saclay, 91198 Gif-sur-Yvette Cedex, France.

[†]These authors contributed equally.

*Address correspondence to: Matias Simons (matias.simons@institutimagine.org).

Abbreviations used: ANOVA, analysis of variance; ATP, adenosine triphosphate; EGFP, enhanced green fluorescent protein; GAPDH, glyceraldehyde-3-phosphate dehydrogenase; mRFP, monomeric red fluorescent protein.

© 2018 Guida, Hermle, *et al.* This article is distributed by The American Society for Cell Biology under license from the author(s). Two months after publication it is available to the public under an Attribution–Noncommercial–Share Alike 3.0 Unported Creative Commons License (<http://creativecommons.org/licenses/by-nc-sa/3.0>).

"ASCB®," "The American Society for Cell Biology®," and "Molecular Biology of the Cell®" are registered trademarks of The American Society for Cell Biology.

and the orientation of hairs toward the distal end of the wing. Current data indicate that there is a set of evolutionary conserved PCP core factors that share the capacity to control polarized hair formation and to localize asymmetrically in cells in so-called PCP domains (Simons and Mlodzik, 2008; Goodrich and Strutt, 2011; Devenport, 2014).

ATP6AP2 shows all the features of a PCP core protein, because 1) loss-of-function experiments cause PCP phenotypes in several *Drosophila* tissues and also other species (Buechling *et al.*, 2010; Hermle *et al.*, 2010, 2013; Schafer *et al.*, 2015), 2) ATP6AP2 interacts physically with other PCP core proteins (Buechling *et al.*, 2010; Hermle *et al.*, 2010, 2013), and 3) shows an asymmetric localization at PCP domains (Hermle *et al.*, 2013). The specific role of ATP6AP2 in PCP is further underscored by the observation that lack of the PCP core factor Flamingo (Fmi) leads to loss of ATP6AP2 at the PCP domains, while the overexpression of Fmi causes a strong accumulation of ATP6AP2 at the cell surface (Hermle *et al.*, 2013).

The molecular basis for the functional diversity of ATP6AP2 is currently unclear. However, it might be linked to a well-described proteolytic cleavage event in the Golgi apparatus that produces an N-terminal and a C-terminal fragment (NTF and CTF, respectively) (Cousin *et al.*, 2009; Zhu and Yang, 2018). While mosaic analysis in flies demonstrated that the NTF from the hemolymph or from the secretion by neighboring cells can localize to PCP domains (Hermle *et al.*, 2013), it was the CTF that copurified with the V-ATPase (Ludwig *et al.*, 1998). Although the knockdown of several V-ATPase subunits has been shown to cause PCP phenotypes (Hermle *et al.*, 2010, 2013), none of the V-ATPase subunits so far examined shares the PCP-like localization pattern of ATP6AP2 or have been shown to be stabilized by Fmi, which may suggest that the V-ATPase function of ATP6AP2 is independent of its function in the PCP pathway.

Here we addressed whether ATP6AP2 also functions as a V-ATPase assembly factor. Using the yeast model, we show that *Drosophila* ATP6AP2 can rescue the impaired growth of *voa1::H vma21QQ* yeast cells. This rescue requires the full-length (FL) sequence and is improved by the coexpression of ATP6AP1. We also demonstrate that the FL protein, and not the cleavage fragments, is required for both PCP and V-ATPase functions in *Drosophila*. Both gain-of-function and loss-of-function of ATP6AP2 causes Xbp1-dependent ER stress. Altogether, the results suggest that ATP6AP2 participates in the assembly of the V-ATPase in the ER and that failure to do so impairs the PCP pathway.

RESULTS AND DISCUSSION

Rescue experiments in yeast

The de novo formation of the multisubunit V-ATPase requires the coordinated assembly of at least 13 different subunits, some of which are present in multiple copies in the complex. In yeast, the assembly of the V0 sector in the ER is facilitated by the assembly factors Vma21, Vma12, Vma22, Pkr1, and Voa1 (Ryan *et al.*, 2008). Recently, mammalian orthologues have been identified for Vma21 (Vma21), Vma12 (TMEM199), and Vma22 (CCDC115) and possibly Voa1 (ATP6AP1) (Ramachandran *et al.*, 2013; Jansen *et al.*, 2016a,b,c). While ATP6AP2 does not exist in *Saccharomyces cerevisiae*, it interacts with ATP6AP1 and possesses a conserved C-terminal ER retrieval motif (Rujano *et al.*, 2017). Therefore, we tested whether ATP6AP2 could function as a V0 assembly factor by expressing FL ATP6AP2 from *Drosophila melanogaster* (ATP6AP2^{FL}; Figure 1A) in *voa1::H vma21QQ S. cerevisiae*, a mutant strain with dysfunctional V0 assembly. In these cells, reduced V-ATPase function can be scored by growth impairment on medium buffered to pH 7.5, media containing high levels of calcium or a combination of both (Ryan *et al.*, 2008). Indeed, ATP6AP2^{FL} expression led to a

significant rescue of the growth impairment of *voa1::H vma21QQ* mutant yeast (Figure 1B). By contrast, this rescue was decreased when expressing the C-terminal fragment (ATP6AP2^{CTF}; Figure 1, A and B) and entirely abolished when expressing an FL version lacking only the short the C-terminal ER retrieval motif (ATP6AP2^{ΔKKXX}; Figure 1, A and B). Moreover, coexpression of its binding partner ATP6AP1 increased the rescue efficiency (Figure 1, A and C). This effect could only be observed when using ATP6AP2^{FL} and not ATP6AP2^{CTF} (Figure 1C), which is consistent with the N-termini of both proteins being responsible for the interaction between both proteins (Rujano *et al.*, 2017). We also expressed both proteins in yeast cells lacking other assembly factors. However, their growth phenotypes could not be rescued, suggesting that ATP6AP1 and ATP6AP2 can specifically replace Voa1 (Supplemental Figure S1).

Restoration of V-ATPase function by coexpression of ATP6AP2 with ATP6AP1 can be visualized qualitatively using quinacrine, a fluorescent dye that accumulates in acidic compartments. *voa1::H vma21QQ* yeast cells are unable to assemble a functional V-ATPase complex and show no accumulation of the quinacrine dye within the vacuoles. However, expression of both ATP6AP2 and ATP6AP1 in *voa1::H vma21QQ* yeast cells demonstrates quinacrine accumulation (bright green disks) similarly to wild-type Voa1 expressing cells confirming the presence of fully functional V-ATPases in the vacuole (Figure 1D). Altogether, these results suggest that in higher organisms a complex of ATP6AP1 and ATP6AP2 has replaced the role of the V0 assembly factor Voa1 in yeast.

Rescue experiments in *Drosophila*

As the V-ATPase assembly function was shown to require the FL protein, we tested whether the FL protein was also needed for viability in *Drosophila*. For this, we generated rescue constructs expressing various ATP6AP2 fragments under the endogenous promoter (FL^{rescue}, NTF^{rescue}, CTF^{rescue}, and ΔC^{rescue}). In the mutant ATP6AP2 background, both NTF^{rescue} and CTF^{rescue} failed to rescue embryonic lethality even when expressed in combination demonstrating that an intact FL protein is essential for survival (Figure 2A). By contrast, ΔC^{rescue} animals died in the late larval stage (Figure 2A) and were thus less viable than ΔKKXX^{rescue} animals, which previously were shown to survive until late pupal stages (Rujano *et al.*, 2017). Both ΔC^{rescue} and ΔKKXX^{rescue} animals showed higher levels of NTF, suggesting that preventing retrograde transport leads to more exposure to Golgi-localized proteases (Supplemental Figure S2, A and B). Interestingly, the insertion of the CTF transgene in the wild-type background was not viable in homozygosity, indicating that it may cause dominant-negative effects. This is consistent with the apoptotic effects and the reduction of endogenous ATP6AP2 at the PCP domains observed on CTF overexpression (CTF^{OE}) in the wing epithelium (Supplemental Figure S3A).

To analyze the rescue efficiency of the deletion rescue constructs on the cellular level, we expressed them in ATP6AP2 mutant clones surrounded by mutant cells rescued by FL^{rescue} (see schematic representation in Figure 2B). Expressing NTF^{rescue}, ΔC^{rescue}, and, particularly, CTF^{rescue} clones led to significantly smaller clones compared with the corresponding FL^{rescue} twin clone (unpublished data), suggesting suboptimal viability or growth (Figure 2C–J). Staining the cell outlines with anti-E-cadherin also revealed that cells expressing NTF^{rescue}, CTF^{rescue}, and ΔC^{rescue} had smaller apical surfaces (Figure 2, D–F). In addition, E-cadherin levels were increased compared with the surrounding wild-type tissue and the FL^{rescue} clones, which is consistent with a reduced lysosomal degradation of E-cadherin and impaired V-ATPase function as shown previously (Hermle *et al.*, 2013). To assess potential PCP phenotypes in the clones, we analyzed actin-based

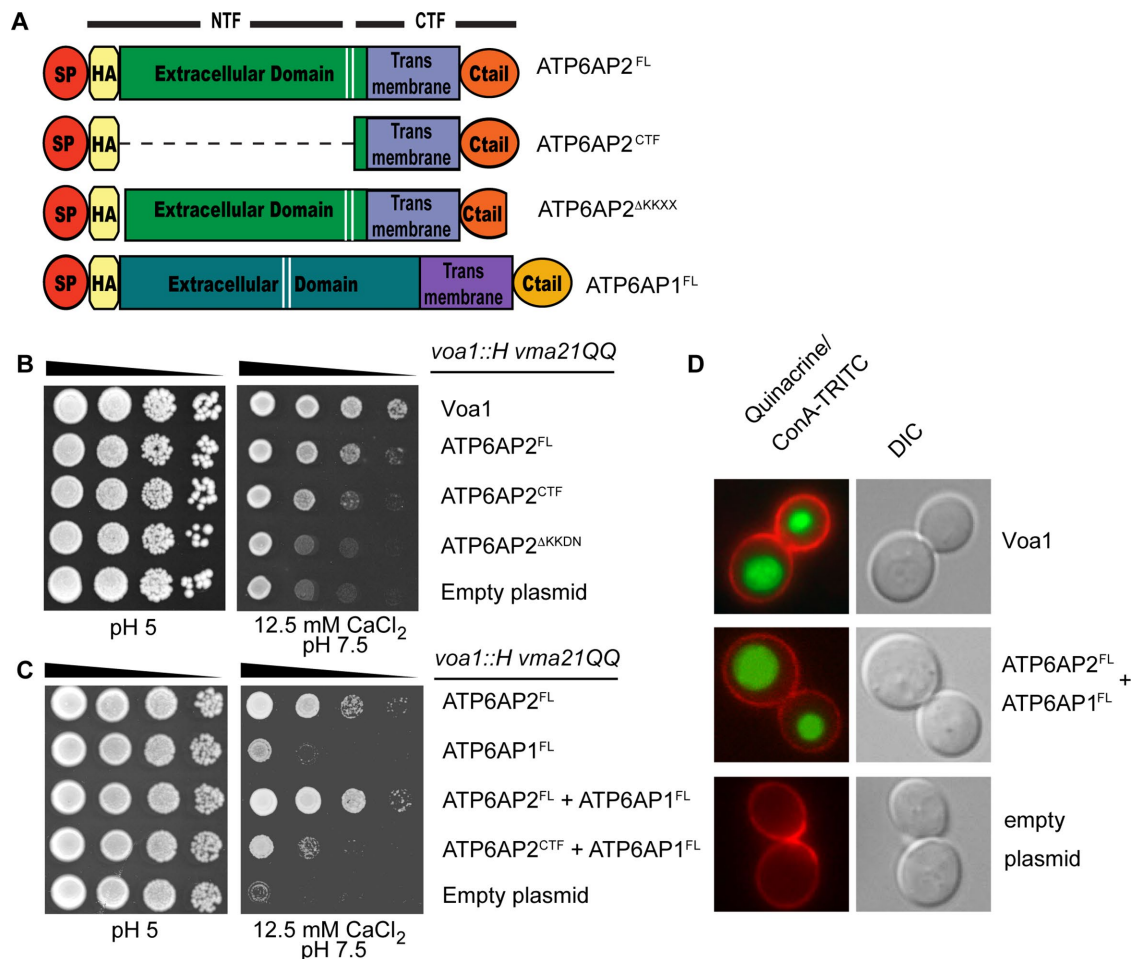


FIGURE 1: Full-length ATP6AP2 can function in place of Voa1 in yeast V-ATPase assembly. (A) Schematic showing fly ATP6AP2 and ATP6AP1 constructs expressed in yeast. All constructs include Voa1 signal peptide (SP) and hemagglutinin epitope tag (HA) followed by ATP6AP2^{FL} (S18-N320), ATP6AP2^{CTF} (D252-N320), ATP6AP2^{ΔKKXX} (pLG496), or ATP6AP1^{FL} (E18-E379). Cleavage at the position indicated by the two white lines generates N- and C-terminal fragments (NTF and CTF, respectively). (B, C) The yeast strain MRY5 (*voa1::H vma21QQ*) was transformed with the indicated plasmids and grown on permissive medium (rich medium buffered to pH 5) and restrictive medium (12.5 mM CaCl₂, pH 7.5) on serial dilution. FL ATP6AP2 rescues Voa1 deficiency better than the CTF alone and requires the ER retention motif KKXX (B). Note that the rescue can be improved by coexpressing fly ATP6AP1 (C). (D) MRY5 yeast cells expressing VOA1 or coexpressing ATP6AP1 and ATP6AP2 were stained with quinacrine and ConA-TRITC. Quinacrine accumulation is depicted in green, and ConA-TRITC marks the outline of the cells in red.

wing hairs. While CTF^{rescue} clones were too small to properly address hair polarity, NTF^{rescue} and ΔC^{rescue} clones showed PCP phenotypes such as multiple wing hairs per cell and misalignment of hairs (Figure 2, G–J). Altogether, these results suggest that despite the strong colocalization of the NTF with Fmi at PCP domains, which is not seen for any of the V-ATPase-associated proteins analyzed so far (Hermle *et al.*, 2013), it is the uncleaved FL ATP6AP2 that is needed for both V-ATPase and PCP functions.



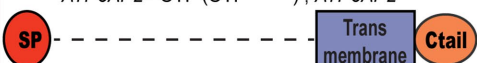
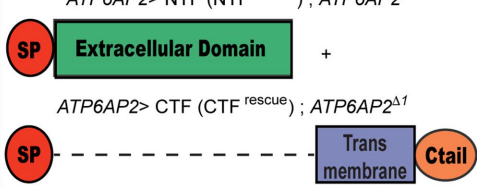

The C terminus of ATP6AP2 mediates ER localization in *Drosophila* wing cells

Next, we analyzed whether ATP6AP2 localized to the ER of wing epithelial cells. Previous experiments had demonstrated that a peptide antibody recognizing a sequence close to the N-terminus mainly detected endogenous ATP6AP2 (or NTF) at the asymmetric PCP domains at the cell surface at steady state (Hermle *et al.*, 2013). This antibody also detected an intracellular pool of ATP6AP2, but this pool was too weak to address any colocalization with ER markers (not shown). By contrast, overexpression of ATP6AP2 using the

wing driver *patched* (*ptc*)-GAL4 showed a strong colocalization with the ER marker protein disulfide-isomerase (PDI) (Figure 3A). Interestingly, PDI was up-regulated in FL^{OE} cells compared with wild-type cells outside the *ptc* compartment, indicating ER stress (Figure 3D). The overexpression of ATP6AP2 ΔC (ΔC^{OE}) and ΔKKXX (ΔKKXX^{OE}) showed less ER localization and reduced PDI up-regulation (Figure 3, B and C), and the overall staining pattern was more vesicular compared with FL^{OE}, particularly for ΔC^{OE} (Figure 3, A–D). Accordingly, we found by Western blotting significantly higher amounts of NTF for both ΔC^{OE} and ΔKKXX^{OE} compared with FL^{OE}, again suggesting increased exposure to Golgi-localized proteases (Figure 3E). Together, these results suggest that the cytoplasmic tail controls ER localization and hence residence time in the Golgi, which in turn affects proteolytic processing of ATP6AP2.

ATP6AP2 overexpression causes ER stress and UPR induction

PDI is commonly up-regulated in the context of ER stress and the unfolded protein response (UPR). An important UPR branch is the

A	Genotype	Lethal stage
	$ATP6AP2 > ATP6AP2$ WT (FL ^{rescue}); $ATP6AP2^{\Delta 1}$	adult
	$ATP6AP2 > NTF$ (NTF ^{rescue}); $ATP6AP2^{\Delta 1}$	embryonic
	$ATP6AP2 > CTF$ (CTF ^{rescue}); $ATP6AP2^{\Delta 1}$	embryonic
	$ATP6AP2 > NTF$ (NTF ^{rescue}); $ATP6AP2^{\Delta 1}$ $ATP6AP2 > CTF$ (CTF ^{rescue}); $ATP6AP2^{\Delta 1}$	embryonic
	$ATP6AP2 > ATP6AP2 \Delta C$ (ΔC ^{rescue}); $ATP6AP2^{\Delta 1}$	third-instar larval

B

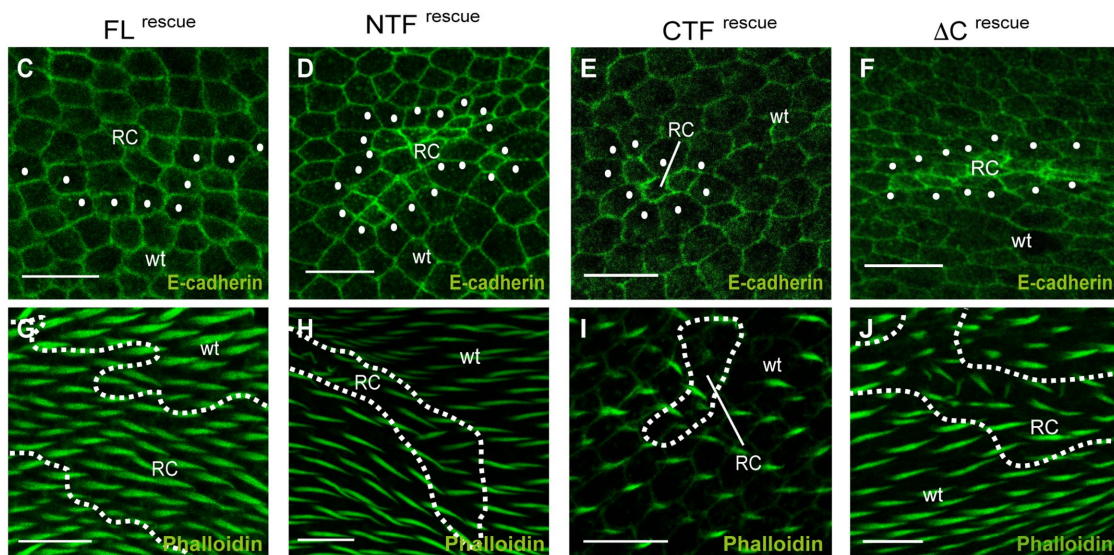
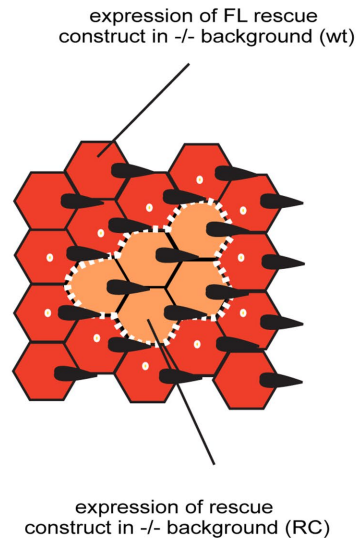


FIGURE 2: Full-length ATP6AP2 is required for survival, PCP, and V-ATPase function. (A) Structure–function analysis using different genomic rescue constructs in an $ATP6AP2^{\Delta 1}$ background. SP denotes the signal peptide of ATP6AP2. Lethal stage is presented on the right side of the table. (B) Schematic diagram of the strategy for mosaic analysis with clones (orange cells; surrounded by dashed white line) expressing rescue constructs (RC) in an $ATP6AP2^{-/-}$ mutant background and surrounding tissue expressing one copy of a wild-type (wt) rescue construct in an $ATP6AP2$ null background (red cells, first row of surrounding tissue marked by white dots). The twin spot (expressing two copies of wt rescue constructs) is not shown. (C–J) E-cadherin (top panel) and phalloidin (bottom panel) staining of clones expressing wt FL (C, G), NTF (D, H), CTF (E, I), or ΔC (F, J) rescue constructs. Note that CTF clones showed a delay in hair growth, but overall clones were too small to assess hair polarity. Scale bars are 10 μ m.

Ire1a/Xbp1 pathway, in which the homodimerizing Ser/Thr kinase Ire1a is able to activate the transcription factor Xbp1 (X-box binding protein 1) by removing one intron from its mRNA. The spliced version of Xbp1 is able to up-regulate ER chaperones, including PDI, by direct binding to stress element promoters in the nucleus (Shen *et al.*, 2001; Yoshida *et al.*, 2001).

To better understand the effect of FL^{OE} on ER homeostasis, we used the xbp1-EGFP reporter, in which EGFP is expressed in frame with Xbp1 only when ER stress-induced splicing occurs (Ryoo *et al.*, 2007). While xbp1-EGFP was not visible on expression of the control protein mRFP (Figure 3F), FL^{OE} caused a high expression of xbp1-EGFP in nuclei of the epithelial cells (Figure 3G), confirming the

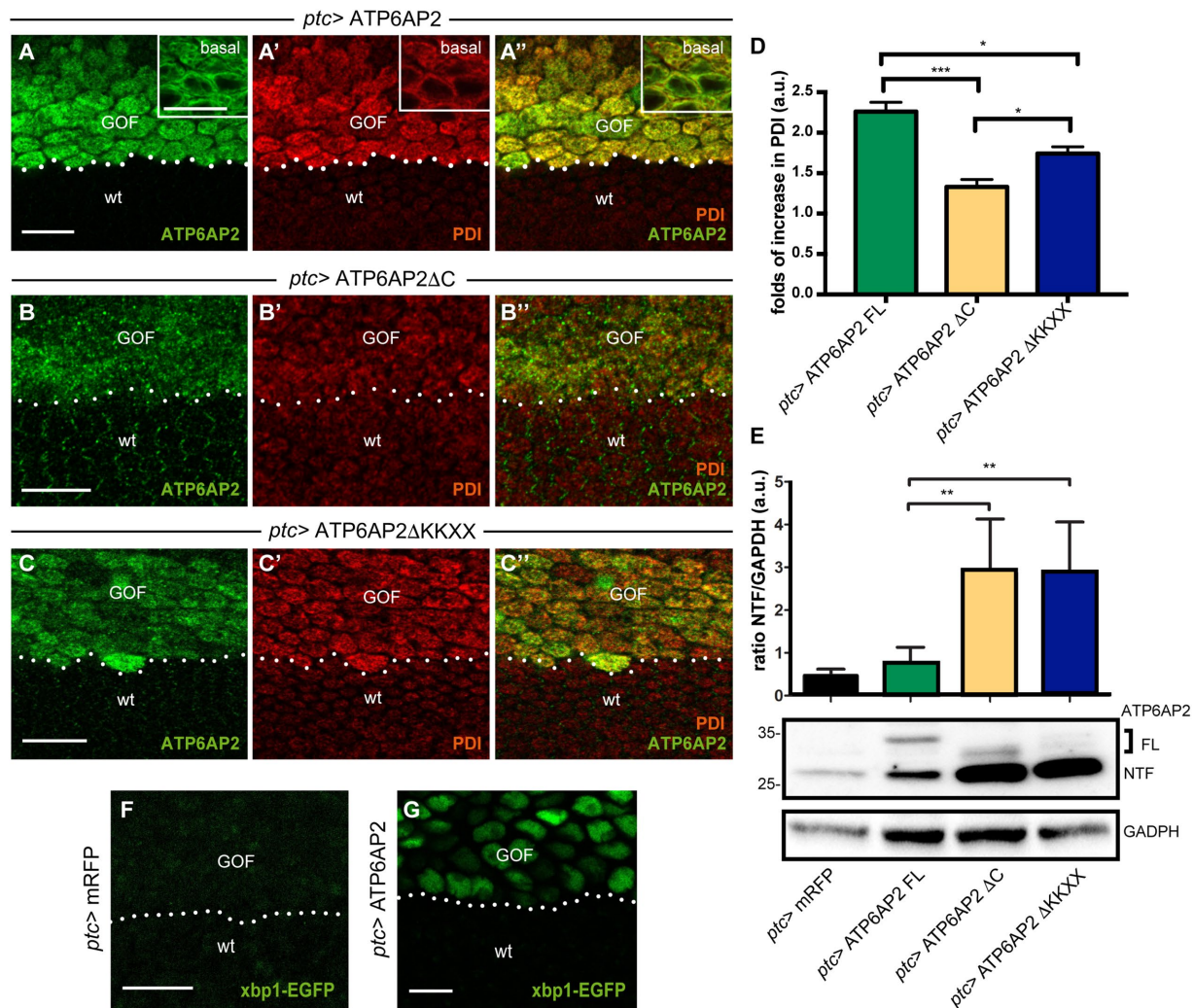


FIGURE 3: The cytoplasmic tail of ATP6AP2 mediates ER localization and ER stress. (A) Overexpressed ATP6AP2 colocalizes with the ER marker PDI (B, B', B"). Gain-of-function (GOF) is performed with the *ptc*-GAL4 driver (expression is above the dotted line), and ATP6AP2 antibody against the N-terminal part was used. ER tubules (marked with PDI) fill the whole cytoplasm and colocalize with ATP6AP2. Note that PDI is strongly up-regulated in ATP6AP2-expressing cells. Insets in A show higher magnification images of more basal areas of the epithelial cells. To avoid saturation of the strong ATP6AP2 signal in the GOF domain, the laser intensity is lower than in B and C (compare also endogenous PCP signal in wt tissue between the different panels). Hence, unlike in B and C, ATP6AP2 staining at the junctional PCP domains is not visible in the wt cells. (B, C) Overexpression of Δ KKXX and Δ C and colabeling with anti-PDI. (D) Quantification of PDI intensity expressed by folds of increased compared with "wt" tissue ($N = 3$ independent experiments, one-way ANOVA, followed by Bonferroni; $*p < 0.05$, $***p < 0.001$). (E) Western blot analysis from pupae homogenates shows increased production of NTF (bottom band) in Δ C and Δ KKXX overexpression. Equal loading was monitored by anti-GAPDH. Quantification of NTF levels, based on densitometry measurements, was done for five independent experiments. Samples from five pupae for each genotype were loaded. $N = 5$ ($**p < 0.01$ by two-tailed *t* test). The data are presented as the mean \pm SD. (F, G) Expression of ATP6AP2 FL (G) with *ptc*-GAL4 (GOF) induced the expression of the UPR reporter Xbp1-EGFP while expression of a control protein (mRFP; F) had no effect. Scale bars are 10 μ m.

induction of the UPR. Interestingly, the expression of both FL^{OE} and Xbp1 RNA interference (RNAi) with *ptc*-GAL4 caused early lethality, suggesting that Xbp1-dependent UPR is essential to counteract the ER stress induced by FL^{OE}.

Overexpression of ATP6AP2 causes V-ATPase and PCP defects in a cytoplasmic tail-dependent manner

To test whether the ER stress caused by FL^{OE} correlated with V-ATPase phenotypes, we used a construct expressing GFP-Lamp1 under the ubiquitous *tubulin* promoter (Pulipparacharuvi et al., 2005). In normal cells, the luminal GFP is targeted to the lysosomes

for degradation, but this does not occur in cells with V-ATPase dysfunction (Hermle et al., 2013). We observed GFP-Lamp1 accumulation in intracellular vesicles in cells expressing FL^{OE} but not with Δ C^{OE} (Figure 4, A and B). This suggests that FL^{OE} has dominant-negative effects on V-ATPase function, possibly by interfering with the precise stoichiometry required for proper V-ATPase function and/or assembly.

With regard to PCP phenotypes, we found that FL^{OE} but not Δ C^{OE} produced cells with multiple wing hairs and mild hair misalignment in adult wings (Figure 4, C and D). Immunostainings of pupal wings showed a slightly less polarized localization for the transmembrane

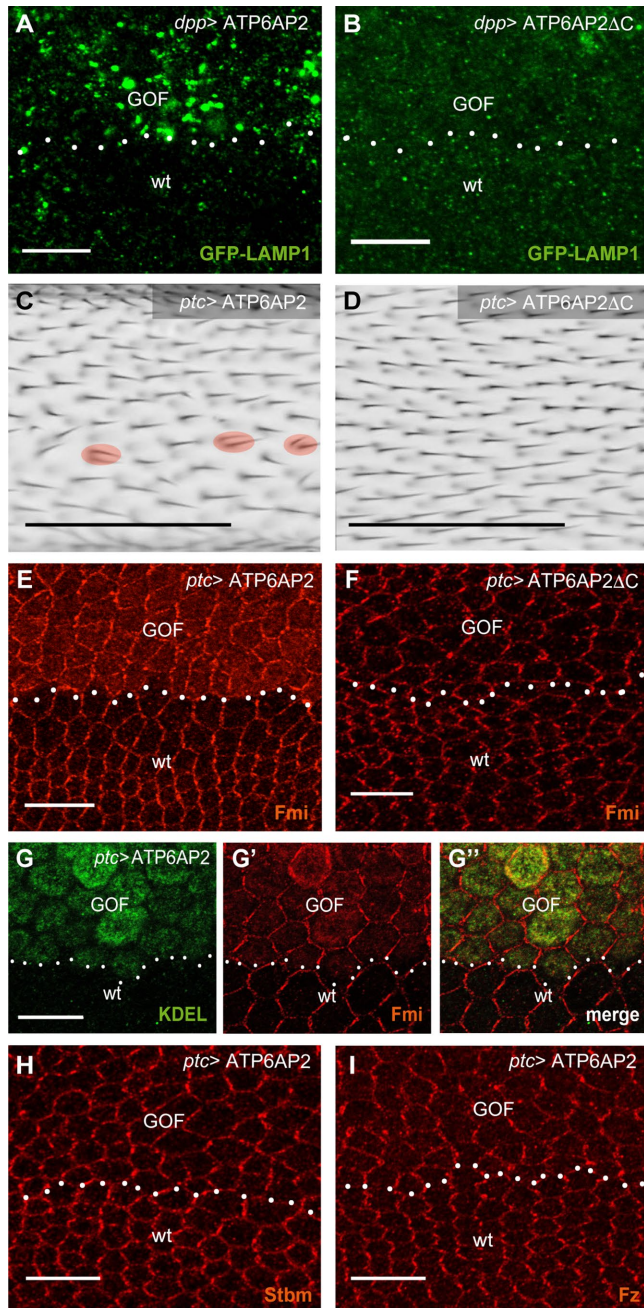


FIGURE 4: Gain-of-function phenotypes depend on the cytoplasmic tail of ATP6AP2. (A, B) ATP6AP2 FL (A) and ΔC (B) overexpression with *dpp*-GAL4 (similar expression domain as *ptc*-GAL4 above dotted line, GOF) caused accumulation of the lysosomal substrate GFP-LAMP1, suggesting a block in lysosomal protein degradation. GFP-LAMP1 is expressed from a direct *tubulin* promoter. Thus, it is also expressed in wt cells outside the *dpp* stripe. (C, D) ATP6AP2 FL (C) and ΔC (D) overexpression in the *ptc* stripe (image taken from a region anterior to the posterior cross vein). Multiple wing hairs per cell are marked with a red circle. (E, F) ATP6AP2 FL (E) but not ΔC (F) overexpression with *ptc*-GAL4 causes intracellular Fmi accumulation. (G) Higher resolution staining of Fmi (G, red) and the ER marker KDEL (G', green). Note that KDEL is like PDI up-regulated by ATP6AP2 overexpression. (H, I) Stbm (H) and Fz (I) do not accumulate in cytoplasm but show slightly reduced asymmetric localization on ATP6AP2 overexpression. Scale bars are 10 μ m for pupal wing stainings and 100 μ m for adult wings in C and D.

PCP factors Frizzled (Fz), Strabismus (Stbm), and Fmi in FL^{OE} cells compared with wild-type cells (Figure 4, E and G–I). Fmi showed an additional intracellular accumulation (Figure 4, E and G). Costaining with the ER marker KDEL showed a partial overlap in the ER, indicating that a subset of Fmi molecules is retained in this compartment via FL^{OE} (Figure 4G). This effect was not seen with ΔC ^{OE}, NTF^{OE}, or CTF^{OE} (Figure 4F and Supplemental Figure S4, A and B). Together, the results suggest that FL^{OE} affects the PCP pathway, at least in part, by causing partial accumulation of Fmi in the ER.

Lack of ATP6AP2 induces ER stress and ER stress is sufficient to cause PCP phenotypes

As overexpression of membrane proteins may cause ER stress in an unspecific manner, we analyzed next whether ER stress was seen in cells lacking ATP6AP2. Indeed, we found increased levels of xbp1-EGFP and PDI on knockdown of ATP6AP2 (Figure 5, A and B). PDI up-regulation was suppressed by the coexpression of Xbp1 RNAi, indicating that ER stress is Xbp1 dependent (Figure 5C). Clones mutant for ATP6AP2 also showed an up-regulation of PDI (Figure 5D), providing additional evidence for the presence of ER stress in cells with too-high and too-low levels of ATP6AP2.

Finally, to address potential links between ER stress and PCP in ATP6AP2-deficient cells, we asked whether the induction of ER stress is sufficient to disrupt PCP. For this, we silenced the ER chaperone BiP, which caused an increase in PDI levels and Xbp1 splicing, as reported previously (Chow *et al.*, 2015) (Figure 5, E and F). In the pupal and adult stage, cells showed severe packing defects, delayed hair growth, and substantial hair misorientation (Figure 5, G and H). Immunostaining for Fmi revealed loss of asymmetry, but no retention in the ER (Figure 5I). Compared with ATP6AP2 knockdown using the same driver (Hermle *et al.*, 2010), these phenotypes obtained by BiP knockdown were thus very similar with respect to Fmi localization and hair orientation but more severe with respect to cell shape regulation and the timing of hair formation (Hermle *et al.*, 2013).

Conclusions

In this study, we show that impairment of V-ATPase assembly caused by a Voa1 deficiency in yeast can functionally be rescued by the expression of fly ATP6AP2. Our data also demonstrate a role of ATP6AP2 in the ER of fly wing cells, indicating that the assembly function is conserved. In both systems, the rescues were dependent on the presence of the NTF and the short cytoplasmic tail containing the ER retrieval motif. As the NTF contains the binding domain for ATP6AP1 (Rujano *et al.*, 2017), it could specifically be required for V0 assembly. However, the ER retrieval motif, which is absent in ATP6AP1, could be important to allow the return of ATP6AP2 and interacting proteins that have escaped to the Golgi or have escorted the newly assembled proton pore to the Golgi, as has been shown for Vma21 (Malkus *et al.*, 2004). When the ER retrieval motif is lacking, ATP6AP2 cleavage is increased (this study and Hermle *et al.* [2013]), suggesting that cleavage in the Golgi could terminate any V0-specific functions of ATP6AP2. Given that mature V-ATPases have been shown to only contain CTFs of ATP6AP1, ATP6AP2, and Voa1 and not the respective FL proteins (Ludwig *et al.*, 1998; Schoonderwoert *et al.*, 2002; Roh *et al.*, 2018), cleavage may also somehow be coupled with the addition of the V1 sectors in the Golgi. However, in the fly at least the rescue with an uncleavable form of ATP6AP2 did not produce any obvious phenotypes (Hermle *et al.*, 2013; Rujano *et al.*, 2017), suggesting that cleavage is not an essential aspect of ATP6AP2 function.

As unassembled V0 subunits have been shown to be targeted for ER-associated degradation (Hill and Cooper, 2000), prolonged

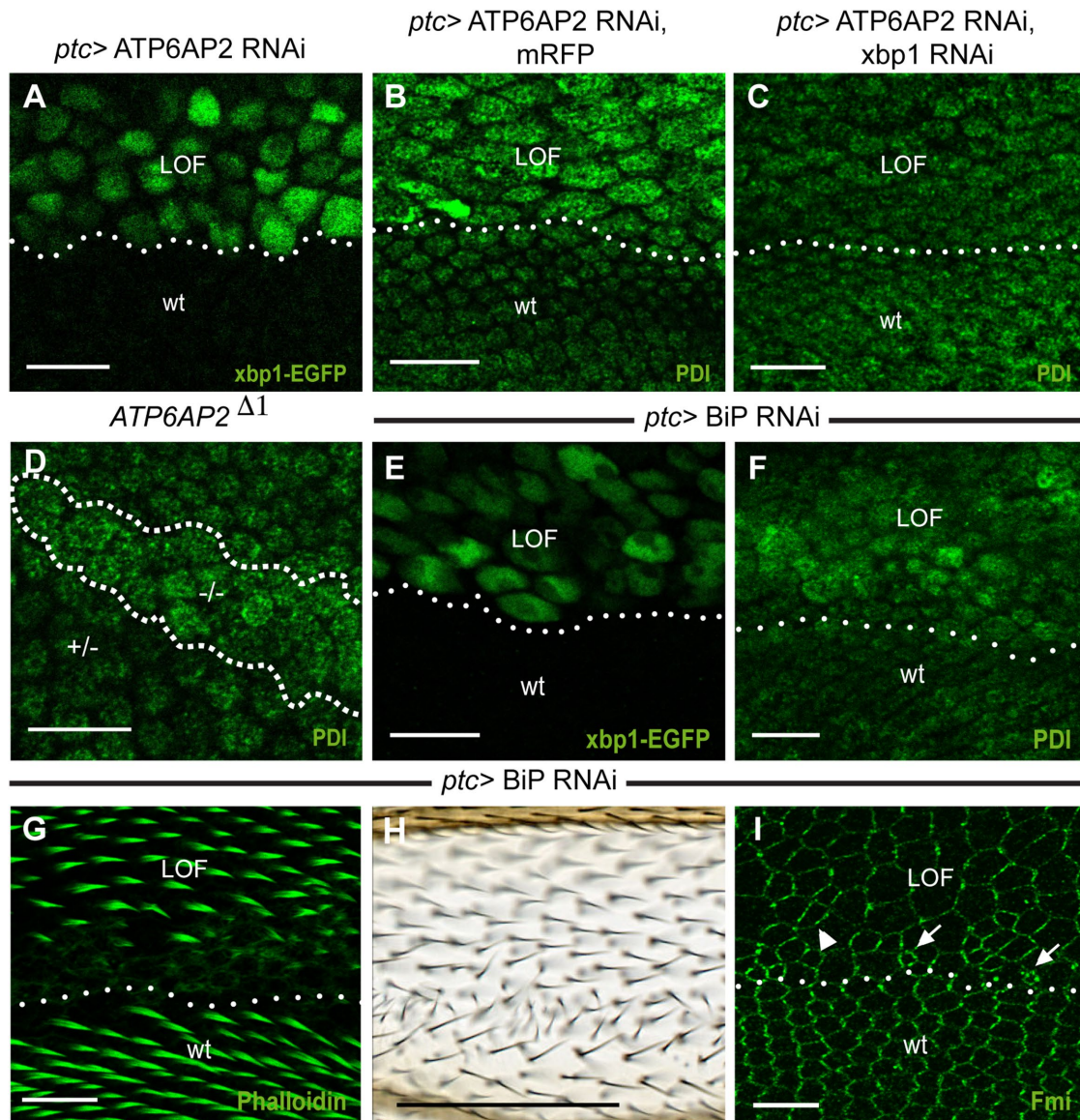


FIGURE 5: ATP6AP2 depletion causes ER stress and ER stress can induce PCP phenotypes. (A) Removal of ATP6AP2 by RNAi using *ptc*-GAL4 (LOF, loss of function; above dotted line) induced Xbp1-EGFP expression. (B, C) Knockdown of ATP6AP2 in the *ptc* stripe (LOF) caused an increase in PDI levels (B) that was prevented by co-overexpression of Xbp1 RNAi (C). (D) Clonal removal of *ATP6AP2* ($-/-$) caused increase in PDI levels (clones were marked by absence of β -gal that is not shown here). (E) Xbp1-EGFP reporter coexpressed with *BiP* RNAi. (F–I) Knockdown of BiP increased PDI levels (F), delayed hair growth, and disrupted hair polarization in pupal (G) and adult (H) wings. (I) Fmi staining on pupal wings on removal of BiP. Note that cells lost their hexagonal shape; instead, they presented a more elongated shape (arrowhead) and irregular cell size (arrows point to small cells). Scale bars are 10 μ m for pupal wing stainings and 100 μ m for the adult wing in H.

misassembly may be directly linked to both V-ATPase dysfunction and ER stress induction (Sekiya *et al.*, 2017). The observation that BiP knockdown caused similar but also different wing phenotypes compared with ATP6AP2 knockdown suggests that part of the PCP phenotypes are ER stress dependent. As the decisive players in PCP are transmembrane proteins that travel through the early secretory pathway while undergoing posttranslational modifications, any disturbance in ER homeostasis could indeed influence signaling at the plasma membrane (Merte *et al.*, 2010; Wansleben *et al.*, 2010). This may be particularly important for the large protocadherin Fmi, which is modified extensively in the ER via glycosylation and autocatalytic cleavage at the G protein-coupled receptor proteolytic site

(Usui *et al.*, 1999; Promel *et al.*, 2012). It can also be speculated that Fmi maturation and V-ATPase assembly could at least in the pupal wing epithelium be linked by common molecular factors in the early secretory pathway where the establishment of PCP requires constant turnover of Fmi in the acidic lysosomes (Strutt and Strutt, 2008; Strutt *et al.*, 2011).

Altogether, we provide evidence that ATP6AP2 functions together with ATP6AP1 in the assembly of the V-ATPase in the ER and that ATP6AP2 can influence PCP signaling at the level of the ER. Additional work is needed to understand by which mechanisms ATP6AP2 can act as a chaperone for PCP proteins in conjunction to its role in V-ATPase assembly.

MATERIALS AND METHODS

Plasmids and yeast strain

Plasmids encoding ATP6AP2^{CTF}, ATP6AP2^{FL}, ATP6AP2^{AKKXX}, or ATP6AP1^{FL} have the same architecture as previous constructs encoding human ATP6AP1 (Jansen *et al.*, 2016a). Briefly, pRS316 vector containing HA-tagged Voa1 with genomic flanking sequence (pMR072) (Ryan *et al.*, 2008) was modified by replacing S26–N265 of the Voa1 ORF with DmATP6AP2^{CTF} (D252–N320), resulting in pMR1503, or with DmATP6AP1 E18–E379, resulting in pMR1701. These plasmids insert fragments were constructed by PCR amplifying yeast codon optimized *D. melanogaster* ds synthetic DNA sequence (gBlocks, Integrated DNA Technologies) with primers having 5' and 3' sequence complementary to pMR072 sequence adjacent to the targeted insertion site. *D. melanogaster* sequence fragments were joined by ligase free cloning (Li *et al.*, 2011) to inverse amplified pMR072 with Voa1 S26–N265 omitted. pMR1608, encoding DmATP6AP2^{FL}, was prepared from pMR1503 by inserting the N-terminal fragment (S18–R251, gBlock) 5' of the D252 codon. pLG493 (pRS415DmATP6AP2^{CTF}) and pLG494 (pRS415DmATP6AP2^{FL}) were generated by subcloning the DmATP6AP2 insert with Voa1 flanking sequence, from pMR1503 and pMR1608, respectively, into pRS415. pLG496 (pRS316 DmATP6AP2^{FL}ΔKKXX) was generated using pMR1608 as PCR template. pMR1608 was inverse amplified using KOD Hot Start DNA polymerase (Novagen) and primers designed to omit C-terminal sequence encoding KKDN and add an EcoRI restriction site immediately following stop codon. For each plasmid, the entire ORF was verified by DNA sequencing. These plasmids all have Voa1 5'UTR, the Voa1 signal sequence (M1–A24) plus the first amino acid after Voa1 signal cleavage (D25), an HA tag followed by the Dm sequence indicated, and Voa1 3' UTR. Plasmids were transformed into *voa1::H vma21QQ* yeast (MRY5: *MATα ura3-52 leu2-3,112 his4-519 ade6 pep4-3 gal2 voa1::HygR vma21QQ::HA*) (Ryan *et al.*, 2008).

Yeast growth assays and quinacrine staining

The ability of the yeast strain MRYS transformed with DmATP6AP2 and/or DmATP6AP1 plasmids to grow at nonpermissive conditions was assayed using a previously described protocol with few exceptions (Jansen *et al.*, 2016a). Liquid cultures of yeast strains with plasmids were grown at 30°C overnight in synthetic media plus dextrose (SD) and supplemented with amino acids (SD-aa) appropriate to select for plasmid(s). Cultures were diluted to 0.5 OD per ml with SD-aa and grown for an additional 6 h. The actively dividing yeast cultures were diluted to 1 OD per ml, and subsequent 1:10 dilutions were made into sterile water. Yeast cells were then spotted onto permissive yeast extract peptone dextrose growth medium (YEPD), pH 5, or nonpermissive agar media of YEPD, pH 7.5, plus 12.5 or 100 mM CaCl₂. Cells were then incubated for 48 h at 30°C prior to growth assay results being recorded.

Quinacrine staining of live yeast cells was conducted as previously described using a final concentration of 200 mM (Conibear and Stevens, 2002). The addition of Concanavalin A tetramethylrhodamine conjugate (ConA-TRITC; ThermoFisher) to final concentration of 50 mM allows fluorescence visualization of the yeast cell surface. Images were acquired using a Zeiss Axioplan 2 fluorescence microscope with a 100× objective and captured using Zeiss AxioVision software.

Fly genotypes

ATP6AP2^{Δ1} and genomic rescue construct was described in Hermle *et al.* (2013). Note that the gene was then termed *VhaPRR*. The new gene name ATP6AP2 that now also can be found in Flybase is adapted to the mammalian nomenclature. For the transgenesis of

rescue constructs and of the upstream activating sequence (UAS) overexpression constructs, *attP* landing sites at cytosite 51C1 and 86F8, respectively, were used (Bestgene). NTF and CTF comprise amino acids 1–248 and 252–320, respectively. See Supplemental Table S1 for a full list of the genotypes used in this study. Primer sequences for cloning into *pattB* and *pUASg.attB*, respectively, are available on request. New lines generated for this study are ATP6AP2 > NTF, ATP6AP2 > CTF, ATP6AP2 > ΔC, UAS-ATP6AP2ΔC, and UAS-CTF. All the others can be found in Hermle *et al.* (2013) and Rujano *et al.* (2017).

Generation of mutant clones

For the clonal analysis, the progeny was heat shocked for 60 min 2–6 d after egg laying, and pupae were staged for immunostainings. Two time points were analyzed: early for immunostaining (28 h after puparium formation [APF] at 25°C or 65 h APF at 18°C) and late for the analysis of pupal wing hairs (34 h APF at 25°C or 72 h APF at 18°C). Clones were recognized by lack of β-Gal staining or in the case of clones expressing the genomic rescue constructs (ATP6AP2 > ATP6AP2 or others) in a null background by lack of expression of mRFP.

Immunostaining of pupal wings

Pupae were dissected in phosphate-buffered saline (PBS). After the pupal case was removed, pupae were fixed with fixation solution (paraformaldehyde 8% in PBS) for 1 h at room temperature (RT). Wings were carefully pulled out of the cuticle and transferred to an Eppendorf with PBS. After three washing steps with PBS–Triton (PBST: 0.1% Triton-X in PBS) wings were blocked for at least 30 min at RT in blocking solution (5% goat serum in PBST) and incubated overnight with primary antibodies diluted in blocking solution. The next day, wings were washed three times with PBST and incubated with fluorescently labeled secondary antibody for 1–2 h at RT. After three washing steps with PBST, the liquid was removed. For the mounting of the pupal wings, Roti-Mount FluoCare (Roth) was added, and wings were placed on a microscope slide with the help of a pipette. Finally, a coverslip was placed on top. Primary antibodies can be found in Supplemental Table S2. Images were taken using a Zeiss LSM 510 META UV confocal microscope or Zeiss LSM 700 confocal microscope. Image processing was performed using ImageJ and Adobe Photoshop CS5 software.

Mounting of adult wings

Adult wings were incubated in isopropanol for 15 min, mounted in Euparal (Roth), and viewed using a Zeiss Axioplan microscope. Nanozoomer 2.0 was used to acquire the images (Hamamatsu). Analysis of the images was performed using NDPview software and Fiji.

Immunoblotting

For Western blots from pupae, white prepupae were collected and aged for 28 h at 25°C. After the removal of the case, three pupae of each genotype were homogenized in 150 μl cold immunoprecipitation (IP) buffer containing 50 mM TrisBase, 50 mM NaF, 150 mM NaCl, 1 mM EDTA, 1% Triton, pH 7.4, and protease inhibitor. For larval lysates, five small third instar larvae were lysed in 100 μl IP buffer. The homogenates were incubated for 30 min on ice and then subjected to 45 min of centrifugation at 13,000 rpm. The supernatant was recovered and 4x Laemmli buffer was added to the samples. Samples were boiled for 3 min at 95°C before loading them onto a 12% SDS–polyacrylamide gel and transfer to polyvinylidene difluoride (PVDF) membranes (Immobilon P; Millipore) by the tank

method within a Mini-Protean 2 Cell chamber (BioRad). Membranes were incubated overnight with the desired primary antibodies at 4°C in Tris-buffered saline, 0.1% Tween 20 (TBS-T) and then incubated with the specific horseradish peroxidase-coupled secondary antibody for 1 h at RT (in 1% bovine serum albumin TBS-T). Bound secondary antibodies were visualized by the enhanced chemiluminescence method (Supersignal West Femto; ThermoScientific). Densitometric quantification of protein expression levels was performed using ImageJ software.

ACKNOWLEDGMENTS

We thank Hermann Steller, Helmut Krämer, Giorgos Pyrowolakis, and the Bloomington Stock Center for fly strains. We thank David Strutt as well as the Developmental Studies Hybridoma Bank for antibodies. We thank Magda Cannata Serio for critically reading the article. The work has been supported by the ATIP-Avenir program, the Fondation Bettencourt-Schueller (Liliane Bettencourt Chair of Developmental Biology), as well as state funding by the Agence Nationale de la Recherche (ANR) under the “Investissements d’avenir” program (ANR-10-IAHU-01) and a NEPHROFLY (ANR-14-ACHN-0013) grant to M.S. and by National Institutes of Health grant GM38006 to T.H.S.

REFERENCES

Buechling T, Bartscherer K, Ohkawara B, Chaudhary V, Spirohn K, Niehrs C, Boutros M (2010). Wnt/Frizzled signaling requires dPRR, the *Drosophila* homolog of the prorenin receptor. *Curr Biol* 20, 1263–1268.

Chow CY, Avila FW, Clark AG, Wolfner MF (2015). Induction of excessive endoplasmic reticulum stress in the *Drosophila* male accessory gland results in infertility. *PLoS One* 10, e0119386.

Conibear E, Stevens TH (2002). Studying yeast vacuoles. *Methods Enzymol* 351, 408–432.

Cousin C, Bracquart D, Contrepas A, Corvol P, Muller L, Nguyen G (2009). Soluble form of the (pro)renin receptor generated by intracellular cleavage by furin is secreted in plasma. *Hypertension* 53, 1077–1082.

Devenport D (2014). The cell biology of planar cell polarity. *J Cell Biol* 207, 171–179.

Forgac M (2007). Vacuolar ATPases: rotary proton pumps in physiology and pathophysiology. *Nat Rev Mol Cell Biol* 8, 917–929.

Goodrich LV, Strutt D (2011). Principles of planar polarity in animal development. *Development* 138, 1877–1892.

Hermle T, Guida MC, Beck S, Helmstadter S, Simons M (2013). *Drosophila* ATP6AP2/VhaPRR functions both as a novel planar cell polarity core protein and a regulator of endosomal trafficking. *EMBO J* 32, 245–259.

Hermle T, Saltukoglu D, Grunewald J, Walz G, Simons M (2010). Regulation of Frizzled-dependent planar polarity signaling by a V-ATPase subunit. *Curr Biol* 20, 1269–1276.

Hill K, Cooper AA (2000). Degradation of unassembled Vph1p reveals novel aspects of the yeast ER quality control system. *EMBO J* 19, 550–561.

Jansen EJ, Timal S, Ryan M, Ashikov A, van Scherpenzeel M, Graham LA, Mandel H, Hoischen A, Iancu TC, Raymond K, et al. (2016a). ATP6AP1 deficiency causes an immunodeficiency with hepatopathy, cognitive impairment and abnormal protein glycosylation. *Nat Commun* 7, 11600.

Jansen JC, Cirak S, van Scherpenzeel M, Timal S, Reunert J, Rust S, Perez B, Vicogne D, Krawitz P, Wada Y, et al. (2016b). CCDC115 deficiency causes a disorder of Golgi homeostasis with abnormal protein glycosylation. *Am J Hum Genet* 98, 310–321.

Jansen JC, Timal S, van Scherpenzeel M, Michelakakis H, Vicogne D, Ashikov A, Moraitou M, Hoischen A, Huijben K, Steenbergen G, et al. (2016c). TMEM199 deficiency is a disorder of Golgi homeostasis characterized by elevated aminotransferases, alkaline phosphatase, and cholesterol and abnormal glycosylation. *Am J Hum Genet* 98, 322–330.

Li C, Wen A, Shen B, Lu J, Huang Y, Chang Y (2011). FastCloning: a highly simplified, purification-free, sequence- and ligation-independent PCR cloning method. *BMC Biotechnol* 11, 92.

Ludwig J, Kerscher S, Brandt U, Pfeiffer K, Getlawi F, Apps DK, Schagger H (1998). Identification and characterization of a novel 9.2-kDa membrane sector-associated protein of vacuolar proton-ATPase from chromaffin granules. *J Biol Chem* 273, 10939–10947.

Malkus P, Graham LA, Stevens TH, Schekman R (2004). Role of Vma21p in assembly and transport of the yeast vacuolar ATPase. *Mol Biol Cell* 15, 5075–5091.

Merte J, Jensen D, Wright K, Sarsfield S, Wang Y, Schekman R, Ginty DD (2010). Sec24b selectively sorts Vangl2 to regulate planar cell polarity during neural tube closure. *Nat Cell Biol* 12, 41–46; suppl 41–48.

Peters J (2017). The (pro)renin receptor and its interaction partners. *Pflugers Arch* 469, 1245–1256.

Promel S, Frickenhaus M, Hughes S, Mestek L, Staunton D, Woollard A, Vakonakis I, Schoneberg T, Schnabel R, Russ AP, Langenhan T (2012). The GPS motif is a molecular switch for bimodal activities of adhesion class G protein-coupled receptors. *Cell Rep* 2, 321–331.

Pulipparacharuvil S, Akbar MA, Ray S, Sevrioukov EA, Haberman AS, Rohrer J, Kramer H (2005). *Drosophila* Vps16A is required for trafficking to lysosomes and biogenesis of pigment granules. *J Cell Sci* 118, 3663–3673.

Ramachandran N, Munteanu I, Wang P, Ruggieri A, Rilstone JJ, Israelian N, Naranian T, Paroutis P, Guo R, Ren ZP, et al. (2013). VMA21 deficiency prevents vacuolar ATPase assembly and causes autophagic vacuolar myopathy. *Acta Neuropathol* 125, 439–457.

Roh SH, Stam NJ, Hryc CF, Couch-Cardel S, Pintilie G, Chiu W, Wilkens S (2018). The 3.5-Å cryoEM structure of nanodisc-reconstituted yeast vacuolar ATPase Vo proton channel. *Mol Cell* 69, 993–1004 e1003.

Rujano MA, Cannata Serio M, Panasyuk G, Peanne R, Reunert J, Rymen D, Hauser V, Park JH, Freisinger P, Souche E, et al. (2017). Mutations in the X-linked ATP6AP2 cause a glycosylation disorder with autophagic defects. *J Exp Med* 214, 3707–3729.

Ryan M, Graham LA, Stevens TH (2008). Voa1p functions in V-ATPase assembly in the yeast endoplasmic reticulum. *Mol Biol Cell* 19, 5131–5142.

Ryoo HD, Domingos PM, Kang MJ, Steller H (2007). Unfolded protein response in a *Drosophila* model for retinal degeneration. *EMBO J* 26, 242–252.

Schafer ST, Han J, Pena M, von Bohlen Und Halbach O, Peters J, Gage FH (2015). The Wnt adaptor protein ATP6AP2 regulates multiple stages of adult hippocampal neurogenesis. *J Neurosci* 35, 4983–4998.

Schoonderwoert VT, Jansen EJ, Martens GJ (2002). The fate of newly synthesized V-ATPase accessory subunit Ac45 in the secretory pathway. *Eur J Biochem* 269, 1844–1853.

Sekiya M, Maruko-Otake A, Hearn S, Sakakibara Y, Fujisaki N, Suzuki E, Ando K, Iijima KM (2017). EDEM function in ERAD protects against chronic ER proteinopathy and age-related physiological decline in *Drosophila*. *Dev Cell* 41, 652–664 e655.

Shen X, Ellis RE, Lee K, Liu CY, Yang K, Solomon A, Yoshida H, Morimoto R, Kurnit DM, Mori K, Kaufman RJ (2001). Complementary signaling pathways regulate the unfolded protein response and are required for *C. elegans* development. *Cell* 107, 893–903.

Simons M, Mlodzik M (2008). Planar cell polarity signaling: from fly development to human disease. *Annu Rev Genet* 42, 517–540.

Strutt H, Strutt D (2008). Differential stability of flamingo protein complexes underlies the establishment of planar polarity. *Curr Biol* 18, 1555–1564.

Strutt H, Warrington SJ, Strutt D (2011). Dynamics of core planar polarity protein turnover and stable assembly into discrete membrane subdomains. *Dev Cell* 20, 511–525.

Supek F, Supekova L, Mandiyan S, Pan YC, Nelson H, Nelson N (1994). A novel accessory subunit for vacuolar H(+)-ATPase from chromaffin granules. *J Biol Chem* 269, 24102–24106.

Usui T, Shima Y, Shimada Y, Hirano S, Burgess RW, Schwarz TL, Takeichi M, Uemura T (1999). Flamingo, a seven-pass transmembrane cadherin, regulates planar cell polarity under the control of Frizzled. *Cell* 98, 585–595.

Wansleeben C, Feitsma H, Montcouquiol M, Kroon C, Cuppen E, Meijlink F (2010). Planar cell polarity defects and defective Vangl2 trafficking in mutants for the COPII gene Sec24b. *Development* 137, 1067–1073.

Yoshida H, Matsui T, Yamamoto A, Okada T, Mori K (2001). XBP1 mRNA is induced by ATF6 and spliced by IRE1 in response to ER stress to produce a highly active transcription factor. *Cell* 107, 881–891.

Zhu Q, Yang T (2018). Enzymatic sources and physio-pathological functions of soluble (pro)renin receptor. *Curr Opin Nephrol Hypertens* 27, 77–82.